

ABSTRACT

We have developed digital 3D Fourier transform methods for comparing the 3D spatial frequency content and hence the axial and transverse resolution of confocal versus conventional microscope images. In particular, we have utilized these techniques to evaluate the performance of our recently-developed confocal transmission microscope for bright field and Nomarski DIC imaging. We have also found that Fourier methods, such as the Hilbert transform, can be successfully employed to overcome the difficulty of visualizing differentially-shaded phase objects, in 3D, that have been acquired using transmission DIC optics.

Keywords: 3D microscopy, confocal transmission DIC, 3D FFT, Hilbert transform, image processing

1. INTRODUCTION

We have recently developed an experimental confocal microscope that can be configured to acquire images in confocal transmission modes, such as transmission bright field and transmission Nomarski differential interference contrast (DIC).¹⁻³ Initial experimental results with this microscope system have shown, particularly when using DIC optics, that a *confocal* configuration (i.e. point-like illumination and detector with pinhole mask) helps reject flare from out-of-focus scattering objects as compared to a *conventional* large-area-detector microscope configuration. In addition, the confocal transmission DIC mode appears to give an improvement in the ability of the system to delineate the edges and surfaces of objects in the axial direction as compared to a conventional DIC microscope. However, these improvements appear visually, in the two-dimensional (2D) optical sections of a confocal focus series, as features that go out of focus more rapidly than in the conventional transmission DIC microscope, rather than as a complete rejection of defocused regions which is the case for all confocal reflection modes.

In this paper, in order to better quantify the performance of confocal versus conventional transmission optical modes, we describe a digital three-dimensional (3D) fast Fourier transform (FFT) method for measuring and displaying the spatial frequencies which comprise our 3D image volumes. In addition, we utilize a Hilbert transform algorithm to extract object features from our 2D transmission Nomarski DIC image slices, in such a way that they can be further processed with a high boost axial filter, and hence clearly visualized as a full 3D volume.

2. FULL 3D FAST FOURIER TRANSFORMS OF 3D DATASETS

Many people are familiar with 2D FFTs applied to everyday image processing tasks. When a 1D FFT is applied to a 2D image the result is an image with a mixture of frequency information in one direction and positional information in the other direction. Such a transform is difficult to interpret and only useful for specialized applications. In a similar way the 2D FFT of a 3D dataset is difficult to interpret because of the non-trivial relation of the positional and frequency components. The 3D FFT of a 3D dataset may still be difficult to interpret, but at least all the axes correspond to spatial frequencies. The 3D FFT is not available on many commercial computer 3D image processing packages. This is perhaps due to the rather excessive (dynamic) memory requirements. We have generated a 3D FFT algorithm by writing some additional sections of C code and compiling them into a commercial software package. This allows us to access the image dataset and 3D FFT it *in situ*, in order to save memory.

If the imaging process satisfies certain constraints (such as being linear and space invariant) then the 3D FFT can be expressed as the product of the object spectrum multiplied by the *optical transfer function* of the imaging process. Thus, in a comparison of imaging processes using the same object, relative responses can be assessed. For example, Figure 1 (left) shows the 3D FFT of a transmission Nomarski DIC image of a thin, lightly stained, biological specimen. Figure 1 (right) shows the 3D FFT of the same object viewed using a transmission bright field mode (i.e. using identical optics except with Wollaston prisms and analyzer removed). The horizontal axes correspond to spatial frequencies in the lateral (x and y) dimensions of the microscope, while the vertical axis corresponds to spatial frequencies in the axial or focus direction (z dimension). The DIC 3D FFT (left) shows a broader (asymmetrical) base than the bright field case. This demonstrates the higher lateral spatial frequency content plus the directional asymmetry characteristic of Nomarski DIC imaging modes. Of particular interest in the renditions of 3D FFTs is the response along the z spatial frequency axis. Components along this axis are indicative of the degree of optical sectioning in the imaging process. Some care has to be taken in interpretation because of the possibility of artefacts arising from image defects such as intensity noise and misregistration (displayed here as strong central peaks).

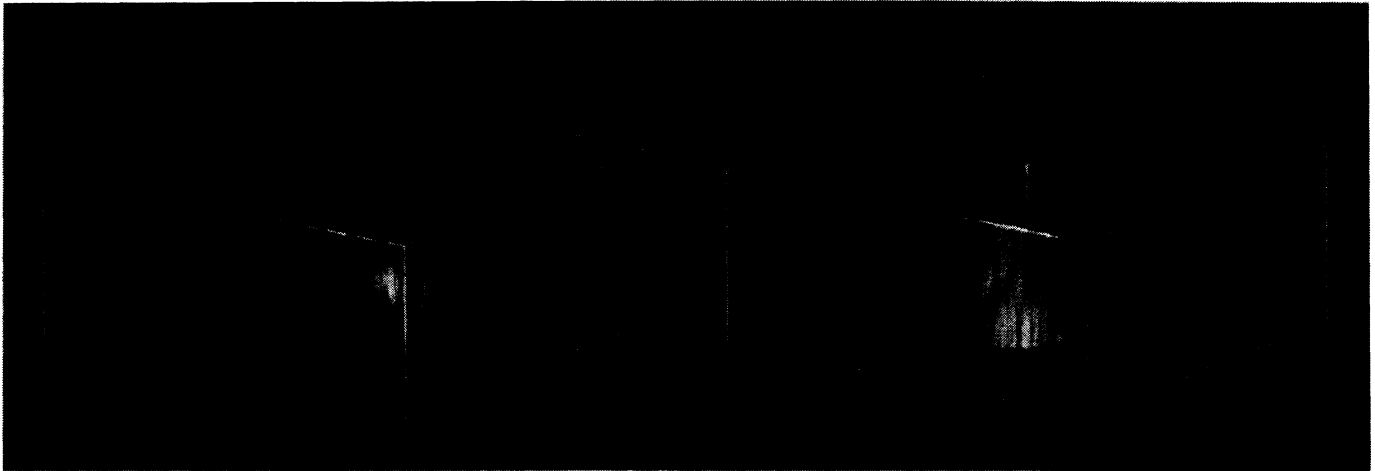


Figure 1. 3D FFTs of transmission Nomarski DIC (left) and transmission bright field (right) image volumes of the same biological specimen (lightly stained orchid root tip chromosomes). Horizontal axes correspond to x and y image spatial frequencies while the vertical axes correspond to axial (z) frequencies. The z axis (vertical scale) has been stretched by a factor of 7 times the x and y scales.

3. 3D VISUALIZATION OF NOMARSKI DIC IMAGES USING THE HILBERT TRANSFORM

3D rendering of image sections obtained using Nomarski DIC produces the following dilemma:

- i) Because Nomarski DIC makes phase structure visible and enhances higher spatial frequency features compared to bright field, it is the preferred transmission optical mode for many biological applications. However, in 2D Nomarski DIC images, the object features appear in *bas relief*, that is to say phase gradients (refractive index boundaries) in the specimen can appear as shadow or highlight (depending on their orientation). This *bas relief* effect produces the visual appearance of 3D, even though the image is obtained from a single plane of focus within the specimen volume.
- ii) Typical digital 3D rendering techniques are based upon controlling either the opacity or the reflectivity of the final displayed image using the total projection of the individual voxel "values" along the

line of sight. Connected segments of a rendered feature are therefore composed of voxels with comparable values. In the case of a transmission DIC focus series, when attempting to render the image data volume in 3D, the shadow and highlight regions of a particular feature will have dramatically different values, hence will not, in general, appear connected.

There are a number of ways around the problem of visualizing 3D Nomarski DIC images. The most obvious is to convert individual DIC image slices back to something resembling bright field. For this method to be of any utility the features gained by Nomarski DIC (such as enhanced high spatial frequencies) must not be lost. The obvious way to convert from Nomarski to bright field is to reverse the (differential) DIC process, i.e., to integrate along the direction of Nomarski shear. This solution has a number of problems which are shown in Figure 2. The image at left is a single 2D slice from a confocal transmission DIC dataset of lightly-stained orchid root tip chromosomes. Figure 2 (middle) shows the result of performing a simple integration operation on the original DIC image. Streaks are due to difficulties initializing the integration. Worse still, the integration process is equivalent to a type of low pass filtering or blurring so that the enhanced high spatial frequencies are lost.

Another way of modelling the Nomarski process is to consider it in the spatial frequency domain. In this system the (real space) differentiation corresponds to *multiplication* by the spatial frequency parallel to the shear. Integration is then just the inverse, namely *division* by the spatial frequency. Both these processes are antisymmetric (or odd) but the division selectively attenuates higher frequency components. What is needed is an antisymmetric transform or process which does not change the relative balance of the various frequency components. Such a transform exists and is known as the Hilbert transform⁴. In essence the transform just keeps all the positive frequency components the same but reverses the sign of all the negative frequency components. The effect of the Hilbert transform on a Nomarski image is shown in Figure 2 (right). The chromosomes which had gray/dark/gray and gray/light/gray shading, on the left and right edges respectively, convert to a lighter central region with dark/light transitions on one side and light/dark transitions on the other side. The main effect is to "symmetrize" the image and render connected regions with similar pixel values.



Figure 2. Comparison of digital processing techniques for confocal transmission Nomarski DIC images. Left: an original confocal transmission Nomarski DIC image of metaphase chromosomes from an orchid root tip preparation. Middle: the resulting image after a computer integration was performed. Right: the resulting image after a Hilbert transform was performed. Chromosome width equals approximately 1 μm .

The implementation of the 2D Hilbert transform (HT) is shown schematically in Figure 3. It is possible to implement an approximate HT in real space^{4, 5} using a special convolution kernel, but we chose the

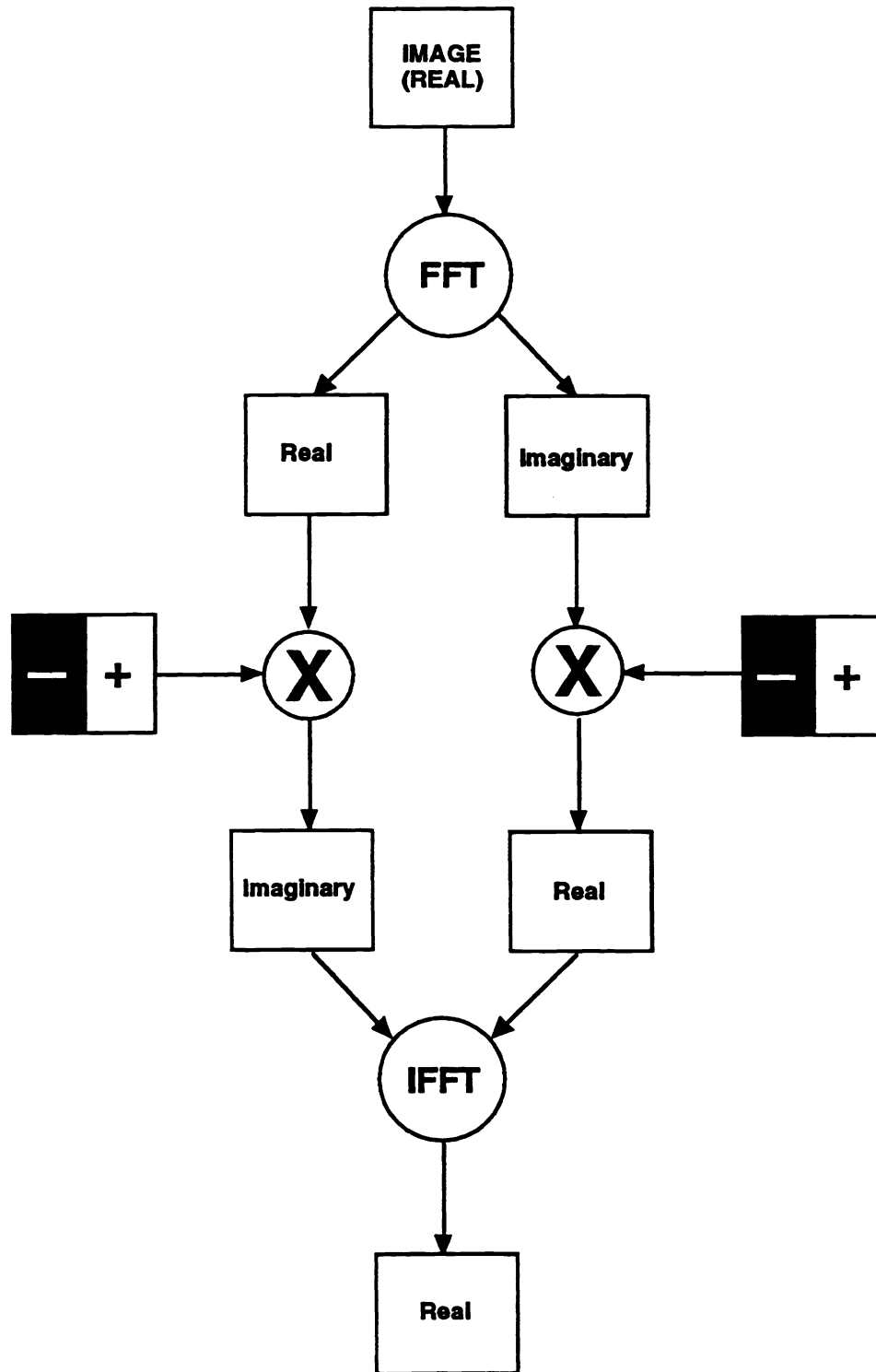


Figure 3 Algorithm for generating Hilbert-transformed Nomarski DIC images

exact method for the images shown in this paper. Briefly the process shown in Figure 3 is as follows:

- Fast Fourier transform (FFT) the image
- Multiply both the *real* and *imaginary* parts of the FFT by the Hilbert frequency response image (which merely consists of +1 or -1 depending on lateral position).
- Swap the resultant real and imaginary parts
- Inverse FFT and take the real part as the new image (the imaginary part is essentially zero).

Once the DIC image slices were Hilbert transformed, we assembled them into a 3D dataset using a volume rendering software package. Next we performed a *high boost* filtering operation which enhanced the high spatial frequencies in the axial direction. Finally, lighting and colour were added and opacity adjusted to improve visibility of the individual chromosomes. Figure 4 shows the results of these image processing steps. At left is a *confocal* transmission Nomarski DIC isometric projection and at right is a *conventional* transmission DIC dataset taken at the same time using the same optics, except that a second, large-area photodetector was utilized and its amplifier gain was increased to match its contrast to that of the confocal detector. Identical image processing and 3D rendering (as described above) were performed on both datasets. The results show that our confocal transmission DIC microscope (left) has more clearly delineated the chromosomes as compared to the conventional case (right) which shows regions where the chromosomes appear smudged.

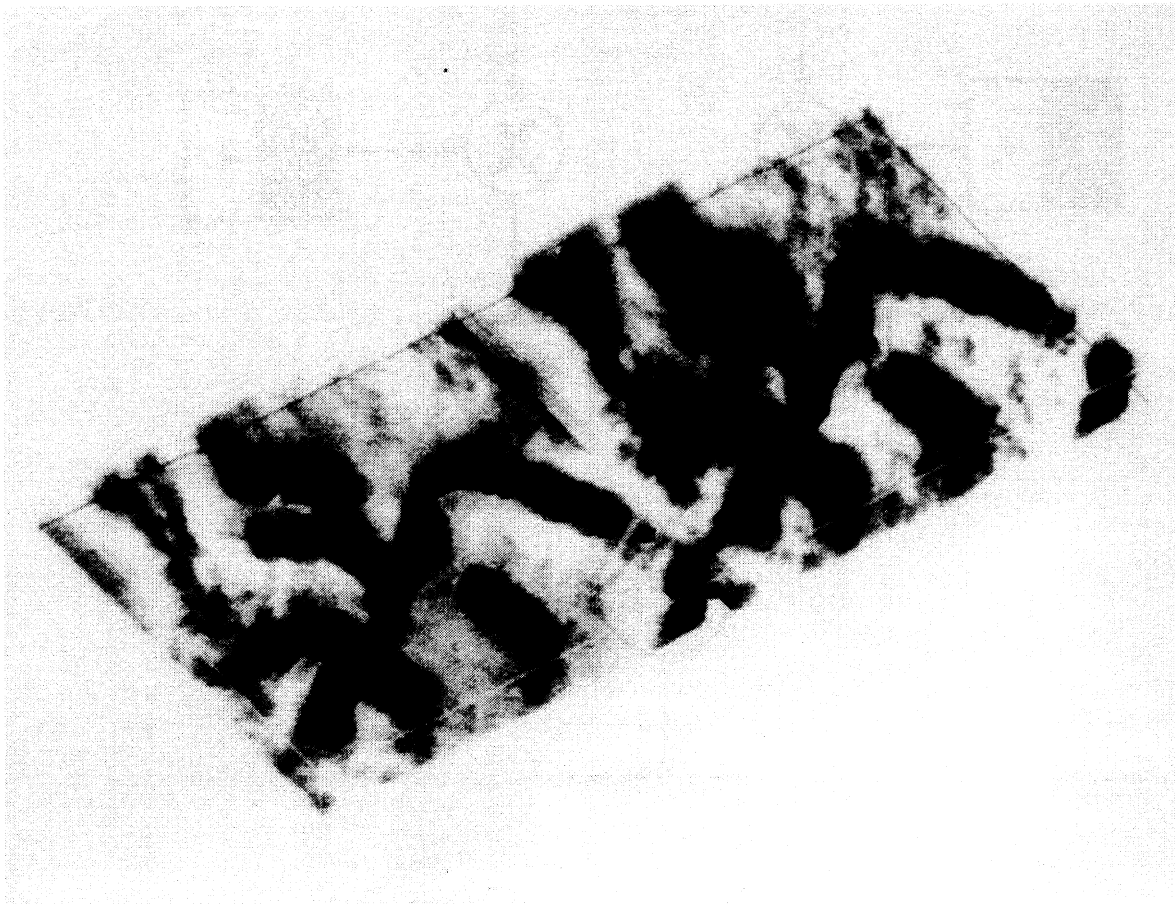


Figure 4. Comparison of confocal (left) versus conventional (right) transmission Nomarski DIC microscopy techniques. These two 3D datasets were acquired simultaneously from the same biological preparation (metaphase chromosomes from an orchid root tip) and were processed and rendered using identical digital imaging methods. The confocal transmission DIC image (left) shows better delineation of chromosomes than the conventional DIC case.

4. CONCLUSION

Utilizing 3D FFT techniques, such as Hilbert transforms and high boost filtering, has allowed us to analyze and evaluate the performance of our confocal transmission microscope as compared to a conventional transmission system. In particular, image processing in the Fourier domain using a Hilbert transform has provided the means by which differentially-shaded Nomarski DIC images can be converted into a form that can be rendered and visualized as a full 3D volume, without losing the enhanced high spatial frequencies characteristic of our confocal transmission DIC microscope.

5. ACKNOWLEDGMENTS

The authors would like to thank the staff of VISLAB (the visualisation laboratory at Sydney University) for help in preparing some of the 3D renditions of the images. The Physical Optics Department is supported by funds from the University of Sydney, the Science Foundation for Physics within the University of Sydney, and the Australian Research Council.

6. REFERENCES

- 1 Cogswell C.J., Larkin, K.G., O'Byrne, J.W. and Arnison, M.R., High-resolution, multiple optical mode confocal microscope: I. System design, image acquisition and 3D visualization. *SPIE* **2184**, 48-54, 1994.
- 2 Cogswell C.J. and O'Byrne J.W., A high resolution confocal transmission microscope: I. System design. *SPIE*, **1660**, 503-511, 1992.
- 3 Dixon, A. E. and Cogswell, C. J., Confocal microscopy with transmitted light, in *Handbook of Biological Confocal Microscopy*, 2nd edition, J. B. Pawley, ed., Plenum, NY, in press, 1995.
- 4 Oppenheim, A., and R, S., *Discrete-Time Signal Processing*, Prentice-Hall, Englewood Cliffs, N.J., 1989.
- 5 Chim, S. S. C., and Kino, G. S., Three-dimensional image realization in interference microscopy, *Applied Optics* **31**, (14), 2550-2553, 1992.